Simulations of a meter-long plasma wakefield accelerator

S. Lee and T. Katsouleas
Department of Electrical Engineering, University of Southern California, Los Angeles, California 90089

R. Hemker and W. B. Mori
Department of Physics, University of California at Los Angeles, Los Angeles, California 90024
(Received 12 July 1999)

Full-scale particle-in-cell simulations of a meter-long plasma wakefield accelerator (PWFA) are presented in two dimensions. The results support the design of a current PWFA experiment in the nonlinear blowout regime where analytic solutions are intractable. A relativistic electron bunch excites a plasma wake that accelerates trailing particles at rates of several hundred MeV/m. A comparison is made of various simulation codes, and a parallel object-oriented code OSIRIS is used to model a full meter of acceleration. Excellent agreement is obtained between the simulations and analytic expressions for the transverse betatron oscillations of the beam. The simulations are used to develop scaling laws for designing future multi-GeV accelerator experiments.

PACS number(s): 52.65.Rr, 52.40.Mj, 41.75.−i

I. INTRODUCTION

In the plasma wakefield accelerator (PWFA), an electron bunch excites a wake in a plasma that can be used to accelerate trailing particles to higher energy. Recently, a PWFA experiment was proposed in which a 30-GeV electron beam at the Stanford Linear Accelerator Center (SLAC) would be used to excite a wake of order 1 GV/m in a meter-long plasma of density $(1-4)\times10^{14}$ cm^{-3}, and the wake used to accelerate the tail of the beam by up to 1 GeV in 1 m. Since the beam in this experiment is typically much denser than plasma (e.g., $N=4\times10^{10}$ electrons in a $\sigma_z=0.6$ mm bunch length and a spot size of $\sigma_r=50$ μm corresponding to a beam density $n_b=1\times10^{15}\,\mathrm{cm}^{-3}$), the PWFA is in the highly nonlinear or blowout regime [1]. This regime offers numerous experimental advantages: a high accelerating gradient, a uniform accelerating structure in the transverse dimensions, very linear focusing, and a high transformer ratio. However, it poses significant challenges for theoretical modeling: inapplicability of linear theory, nonlaminar plasma motion or ''sheet crossing'' that leads to the breakdown of fluid models, and highly localized plasma density spikes. In this paper we describe a comprehensive effort to model a meter-long PWFA in this highly nonlinear regime with two-dimensional (2D) particle-in-cell simulation models. The simulations support the design of the proposed experiment, elucidate some of the important physical phenomena such as betatron oscillations of the beam, and provide scaling laws for designing future experiments to reach 10–100-GeV energies.

The remainder of the paper is organized as follows: In Sec. I, we describe the parameter regime of the PWFA and the experiment to be modeled. In Sec. III we describe the various simulation tools used in the paper, and compare sample results from each. In Sec. IV results are presented from runs modeling short distances typically less than 1 cm (i.e., the initial wake response). The dependence of the wake response on physical parameters such as beam number, plasma density, beam radius, plasma radius, etc. are presented. In Sec. V, results of meter-long runs are presented showing the effect of betatron oscillations of the beam. In Sec. VI, the possible extension of the mechanism to yet higher acceleration gradient and energy is explored.

II. DESCRIPTION OF SAMPLE PROBLEM

In this paper we consider the plasma wake excited by a symmetric drive bunch in the nonlinear or blowout regime [2,3]. A cartoon illustrating the wake generation mechanism is shown in Fig. 1. The modeling is motivated by the parameters of the PWFA experiment (E-157) at the SLAC. The nominal design parameters for this example are given in Table I along with the corresponding simulation model parameters. The experimental beam conditions modeled are $N=4\times10^{10}$ electrons, beam radius $\sigma_r\cong75\,\mu$m and bunch length $\sigma_z\cong0.6$ mm. For the beam distribution we first used experimental data from previous SLAC runs [1], and later used an approximate Gaussian fit to the distribution. Figure 2 shows the Gaussian and measured SLAC beam distributions. The simulations showed no appreciable difference between the case of the actual distribution and the Gaussian fit; accordingly throughout this paper, all the simulations were done with a Gaussian beam distribution.

For comparison to the simulations to follow, here we give an approximate expression form 2D linear theory expression for the plasma wake from a symmetric Gaussian bunch [4]:

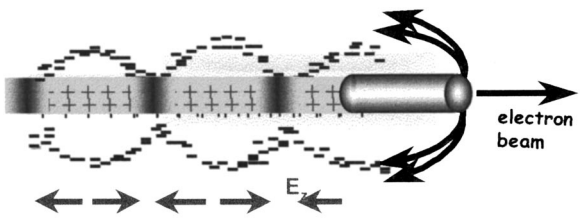

FIG. 1. Physical mechanism of the plasma wakefield accelerator. The space charge of a driving beam displaces plasma electrons. Plasma ions provide a restoring force that leads to a plasma density wake.

TABLE I. Particle-in-cell (PIC) simulation parameters for the beam and plasma.

Beam	number *(N)*	4×10^{10}
	length (σ_z)	0.6 mm
	radius (σ_r)	5–75 μm
	emittance	$\gamma\varepsilon<60$ mm mrad
Plasma	density (n_o)	$(1-10)\times10^{14}$ cm^{-3}
	Ion/e^- mass ratio	5400
	Width	50–500 μm
Simulation	Cell size	$(0.01-0.05)c/\omega_p=0.36-18$ μm
parameters	Number of cells in z	500–2500
	Number of cells in r	200–1000
	Particles in cell	9

$$eE_g \approx \sqrt{n_o}\ \text{ eV/cm}\times\frac{n_b}{n_o}\frac{k_p\sigma_z e^{-k_p^3\sigma_x^2/2}}{1+\frac{1}{k_p^2\sigma_r^2}}$$

$$\approx 80\ \text{ MeV/m}\times(N/10^{10})\times(0.6\ \text{ mm}/\sigma_z)^2, \qquad (1)$$

where we have substituted nominal values ($\sigma_r=75\,\mu$m) from Table I and $2\sigma_z\approx\pi(c/\omega_p)$ to obtain the last expression.

We note that the validity of linear theory requires $n_b \ll n_o$. From the table of parameters above, this condition is violated (3.4, for $\sigma_r=75\,\mu$m). Nonetheless, as we will show, the above scaling law is a useful guide.

III. DESCRIPTION AND COMPARISON OF SIMULATION MODELS

Particle-in-cell (PIC) models of plasma accelerators have been benchmarked against laser-plasma accelerator [5] and particle beam driven (PWFA) experiments [6], and shown to provide reliable description of complex plasma behavior. In the highly nonlinear blowout regime of interest here, analytical and numerical descriptions are quite limited and we rely on the PIC approach. The PIC method computes the motion of a collection of charged particles interacting with each other through fields determined from a self-consistent solution of Maxwell's equations on a grid.

We have been using several PIC codes and algorithms for modeling the PWFA. These are MAGIC, PEGASUS$_C$, and OSIRIS. MAGIC [7] is maintained by Mission Research Corporation. It has a two-dimensional cylindrically symmetric algorithm, which has a charge-conserving current deposition scheme [8]. The computation is done on a fixed grid, i.e., stationary window, and it is not parallelized. Therefore, its use is limited for studying the PWFA in which a bunch propagates through long regions of plasma. PEGASUS [9] uses a charge-conserving scheme from ISIS [10], and it has a moving window algorithm so that it can in principle be used to model the drive beam propagation through meter-long distances. PEGASUS$_C$ is a serial version of PEGASUS with a cylindrically symmetric coordinate system. OSIRIS [11] is a newly developed object-oriented multidimensional (two- or three-dimensional) parallel PIC code written in FORTRAN90. It has a parallelized moving window algorithm and options for two charge-conserving current deposition algorithms [8]. Recently, the cylindrically symmetric algorithm from PEGASUS was incorporated into OSIRIS. The use of parallelism reduces the time for a full meter simulation from 17 days (using PEGASUS) to 1–2 days (using OSIRIS). The reader is

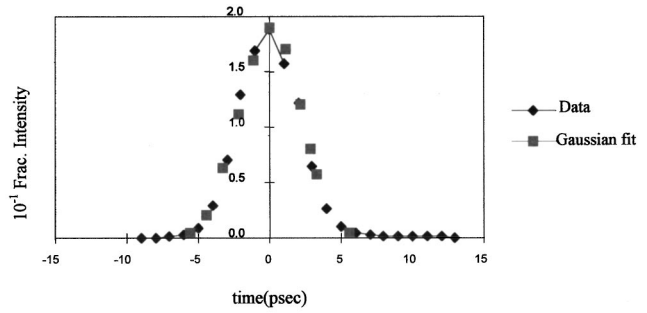

FIG. 2. Comparison of measured SLAC longitudinal beam profile and a Gaussian fit.

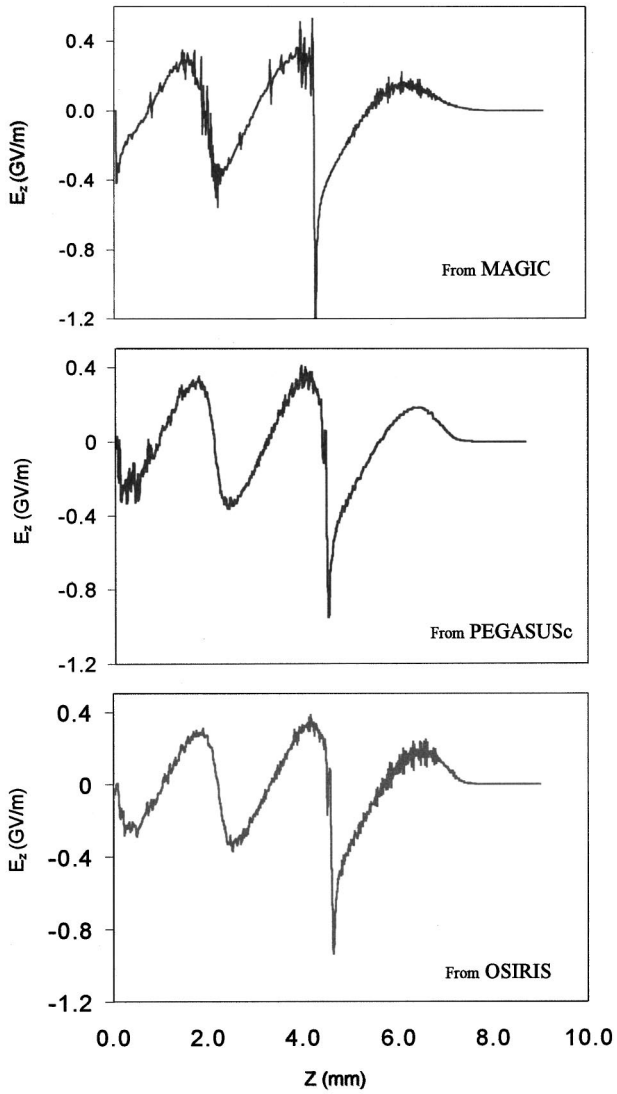

FIG. 3. Comparison of longitudinal wakefields E_z vs z from three different PIC codes: (a) MAGIC, (b) PEGASUSC, and (c) OSIRIS. The cell size was $0.05c/\omega_p$ and the number of particles per cell was nine for each. The beam centers in each graph are at 5.72, 4.7, and 6.61 mm, respectively.

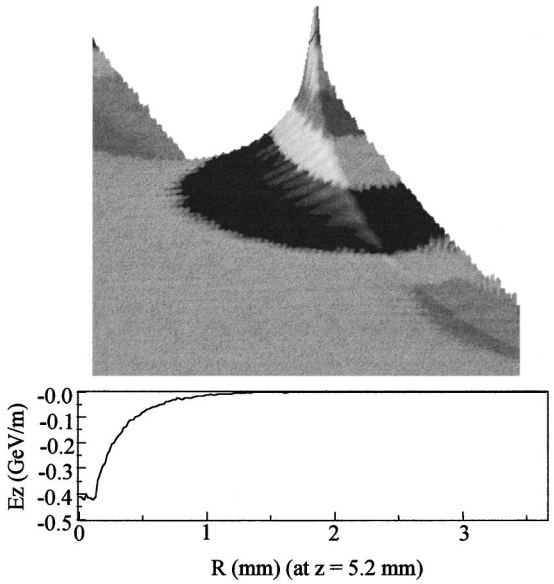

FIG. 4. 2D rubber sheet image of E_z vs z and r (direction out of page), and (below) a slice plot at $z=5.2$ mm for the case in Fig. 3(a).

referred to the references above for more detailed descriptions of the algorithms.

In Fig. 3 we compare the plasma wake, E_z vs z, yielded by each of these codes for the parameters given in Sec. II (except as noted in the figure caption). In each case, the electric field first rises at the head of the beam to a peak decelerating field of 200 MeV/m then drops rapidly to form a narrow spike with a value near -1 GeV/m. We comment that the transformer ratio for this case, the ratio of the accelerating and decelerating fields is nearly 5. This exceeds the fundamental wakefield theorem limit (for symmetric bunches) of two [12]. This will be discussed later. Fairly good agreement is obtained between the codes for similar numerical parameters. Some differences are seen in the shape of the wake behind the first spike and in the noise level. We have also compared other field and plasma quantities (not shown) with similar results from each code.

In Fig. 4 a rubber sheet image of E_z vs r and z and a lineout of E_z vs r at $z=5.2$ mm (corresponding to the simulation in Fig. 3) is shown. The flattening of E_z vs r characteristic of the blowout regime is apparent. In the rubber sheet image the boundary of the blowout region is visible as a faint ridge [13,14].

We also explored the sensitivity of the results to numerical resolution. In Fig. 5 we show the plasma wake from OSIRIS runs for several values of the grid size and 5×5 particles per cell. We find that, except for the spike, the results are insensitive to grid size in this range. However, the amplitude of the spike is not resolved and the spike is smaller in the coarse resolution runs.

For comparison to the PIC results, in Fig. 6 we also show a corresponding run with a nonlinear fluid model, NOVOCODE [15]. The fluid model resembles the PIC results up to the peak-accelerating field (where it is typically broader and smaller). At the spike in the field, plasma fluid elements are clearly crossing, as seen in the real space plot of plasma electrons in Fig. 7. Since the crossing of fluid elements causes singularities in the fluid description, the fluid model breaks down at this point, accounting for the discrepancy between Figs. 3 and 6.

IV. MODELING OF SHORT DISTANCES (EARLY WAKE RESPONSE)

To determine the optimal beam and plasma conditions for the experiment as well as to test the sensitivity of the experiment to variations in the plasma and beam parameters, we have performed a number of simulations surveying param-

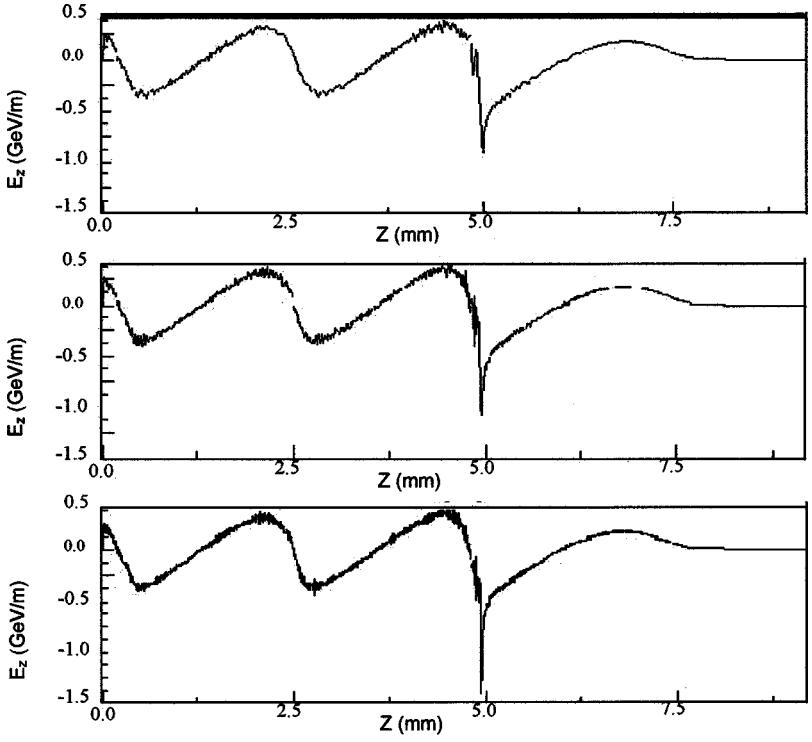

FIG. 5. Longitudinal wakefields in OSIRIS for various spatial resolutions. Cell sizes $dz=dr$ $=$ (a) $0.05c/\omega_p$, (b) $0.025c/\omega_p$, and (c) $0.01c/\omega_p$. There are nine particles per cell in each case.

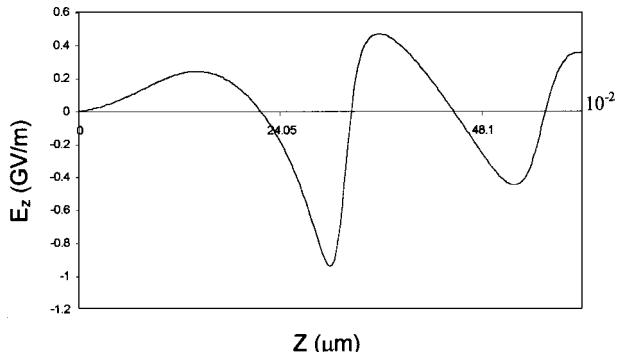

FIG. 6. Longitudinal wakefield E_z vs z in a nonlinear fluid code NOVOCODE simulation. Parameters are as in Table I, and the beam center is at $z=1.5$ mm.

eter space. Except where otherwise noted the simulations in this section were done with the code MAGIC. The results are summarized in Figs. 8–11. Figure 8 shows the dependence of the peak wake amplitude on the plasma density. The peak is 900 ± 100 MeV/m at a plasma density of 2.1×10^{14} cm^{-3}. The uncertainty quoted is due to numerical noise. The peak corresponds approximately to a beam width of $2\sigma_z$ matched to $\pi c/\omega_p$. At lower densities there is not enough plasma to support large wakes, while at higher densities $\pi c/\omega_p$ becomes short compared to the bunch length and the plasma ''shorts out'' the space charge field of the beam. Also shown are the numbers of particles accelerated vs plasma density (i.e., the number of the particles in the tail of the beam that witness an accelerating field larger than $>70\%$ of the peak wake amplitude). We comment that the wakefield response is very sensitive to the bunch length. Shorter bunches give much larger gradients and correspond to higher optimal plasma densities. For example, for a Gaussian bunch with $\sigma_z\approx0.4$ mm, the peak gradient is 2.5 GeV/m at a density of 10^{15} cm^{-3}. This scaling will be discussed further in future work. Figure 9 shows the dependence of wake amplitude on number of beam particles. The amplitude scales nearly linearly in beam number. Figure 10 shows the sensitivity of the wakefield to the beam spot size. As expected, the wake amplitude changes very little with spot size for beam sizes much smaller than c/ω_p.

Since the plasma for the experiment will be produced by a laser of finite spot size, we also simulated the effect of different plasma widths on wake production. For our nominal beam parameters, we find that wake amplitude begins to degrade for plasmas narrower than 300 μm in radius (Fig. 11).

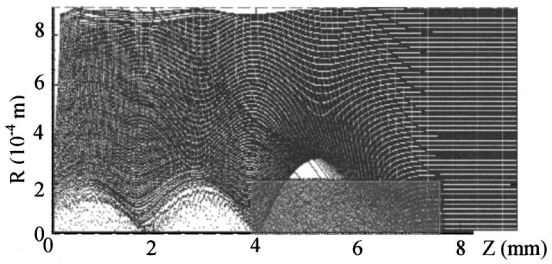

FIG. 7. Real space of plasma and beam electrons. Note that the beam charge density is Gaussian, not rectangular as it appears. The charge on each electron is not the same.

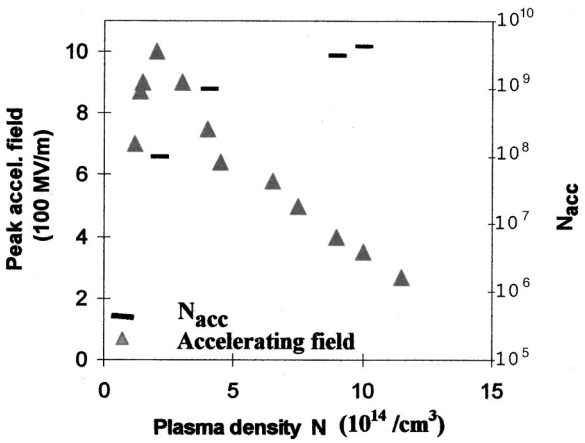

FIG. 8. Wake amplitude vs plasma density and approximate number of accelerated particles experiencing accelerating fields greater than 70% of the maximum gradient.

This corresponds roughly to the maximum outward excursion one would calculate for the plasma electrons ejected by the beam [16]. The outward excursion can be estimated as twice the equilibrium channel radius (r_c) that would result from a balance of electron beam space charge and ion plasma space charge. This radius is $r_c=\sigma_r\sqrt{n_b/n_o}$. The factor of 2 comes from electron inertia. For our example, $\sigma_r=75\,\mu$m and $n_b/n_o=3.38$, giving $2r_c\sim270\,\mu$m. This is roughly in agreement with the plasma radius below which the wake amplitude begins to decrease.

As noted in Sec. III the transformer ratio obtained from any of Figs. 2, 5, or 6 is significantly larger than 2, the limit given by the fundamental wakefield theorem [17]. This is an interesting consequence of nonlinear plasma dynamics in this blowout regime, and we discuss it briefly here. The transformer ratio can be measured in the plots of E_z vs z as the ratio of the peak value of the accelerating electric field (i.e., the spike) to the peak value of the decelerating field in the region ahead. From the graphs, this ratio is approximately 4–5. The fundamental wakefield theorem, on the other hand states that for symmetric colinear bunches in a regime in which linear superposition applies, the transformer ratio can never exceed 2. This limit is easily exceeded by using asymmetric bunches for which the current rises more slowly at the head and falls quickly at the tail (i.e., ramped profiles [18]). In the cases studied here, the bunches are symmetric, but the

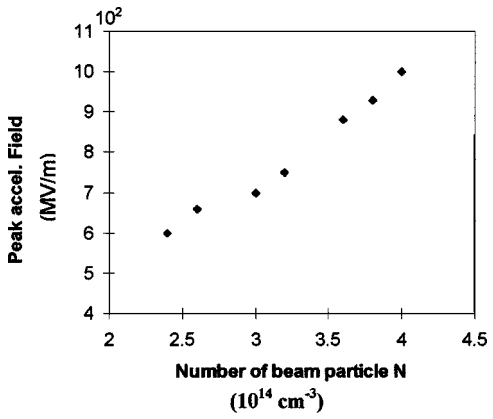

FIG. 9. Wake amplitude vs number of beam particles.

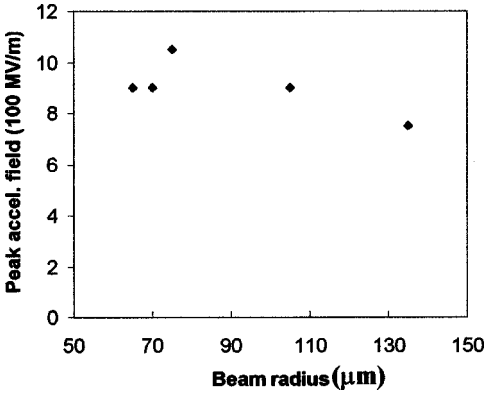

FIG. 10. Wake amplitude vs beam radius.

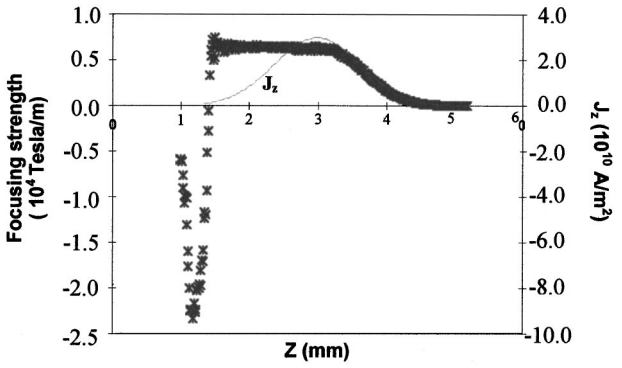

FIG. 12. Focusing strength $(E_T - B_\theta)/r$ at $r=\sigma_r$ vs z. Also shown is the longitudinal current density distribution.

fundamental wakefield theorem does not apply because the wakefield response is nonlinear. It is interesting to point out a similarity between the nonlinear symmetric bunches and the linear ramped bunches. The argument is as follows: While the head of the bunch sees a local plasma frequency ω_p, as usually defined, the relativistic mass increase of blown out plasma electrons effectively lowers the (local) plasma frequency seen by the tail of the bunch. In units of the local plasma frequency, the tail is then shorter than the head. The beam then somewhat resembles a ramped beam with a correspondingly larger transformer ratio.

Before moving on to the longer simulation runs, we briefly describe the transverse wake. In Fig. 12 we show a slice plot of $(E_r - B_\theta)/r$, the transverse wake (proportional to the focusing force on a beam electron), as a function of z at a radius of $r=75\,\mu$m. Note the flattening of the curve behind the head of the beam (once blow out has occurred). The size of the focusing force in this region is approximately 6000 T/m, which is in nice agreement with the expected value [16]. The expected value is simply the radial electric field of a uniform ion column of density equal to the plasma density: $eE_r = 2\pi n_o e^2 r$. For our example, with $n_o = 2.1\times 10^{14}\,\mathrm{cm}^{-3}$, $E_r/r \sim 6.3\times 10^5$ statvolt/cm$^2 \sim 6300$ T/m.

V. MODELING OF A METER-LONG PWFA

The computing time required for the fixed frame simulations of Sec. IV is typically 45 min on an RS6000 workstation (approximately 60-μs/particle time step$\times 10^5$ particles $\times 450$ time steps).To model the full meter-long experiment in this way would require 100 times as many particles and 100 times as many steps. In order to model the full meter within the limitations posed by current computing speeds, we took the algorithms for cylindrically asymmetric PIC code simulations and implemented them into the objected-oriented code OSIRIS with FORTRAN90. This object-oriented programming handles different aspects of problem in different modules (classes) that communicate through well-defined interfaces. This makes it easy to extend the code to include new algorithms without losing any of its previous functionality.

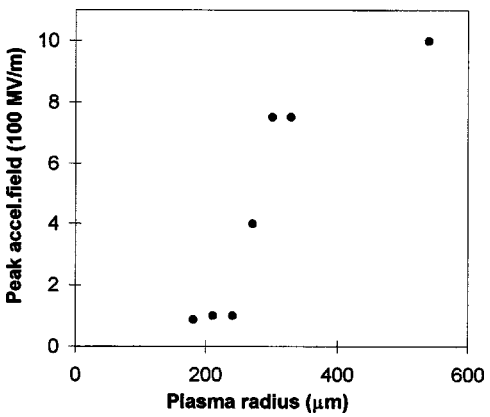

FIG. 11. Wake amplitude vs plasma radius.

By implementing the cylindrically symmetric algorithms into OSIRIS, we were able to take advantage of two advanced features that lead to a considerable speedup of the simulations. First, OSIRIS has a moving window feature that allows the simulated area to move together with the beam that is propagating at the speed of light. This is not a physical transformation into the frame of the beam, but a reuse of computer memory that is possible because all the physics of interest takes place in the area of the beam and a couple of plasma wavelengths behind it. As the beam moves into new plasma in front of it the information about the plasma that falls too far behind the beam is discarded, and the freed up memory can be reused. For the PWFA simulations this means that effectively only about 10 mm of plasma have to be simulated rather than 1 m. This is a savings factor of 100. Second, OSIRIS is a parallel code that allows for domain decomposition of the problem in any number of dimensions. For the simulation of a 1-m PWFA we ran the code on ten nodes of a Cray T3E, which led to a turnaround time of less than two days for propagation through the full 1 m of plasma. The simulations used about 6×10^5 particles and 1.4×10^5 time steps.

Figure 13 shows results of a meter-long run. Snapshots of the accelerating wake along the axis are plotted at distances corresponding to the first minimum and maximum of the betatron oscillations and at 100 cm into the plasma. Also shown in Fig. 14 are snapshots of the electron bunch in real space at the same distances into the plasma. The betatron oscillations of the beam due to the radial focusing force of the plasma ions are clearly visible. Despite the betatron oscillations, the wake is seen to change very little over this distance. This can be understood since the relativistic bunch does not distort longitudinally and the wake is relatively insensitive to radial motion of the beam as seen from Figure 11 (E_z vs beam radius). The wavelength of the betatron oscillations of the middle and tail part of the beam is given by

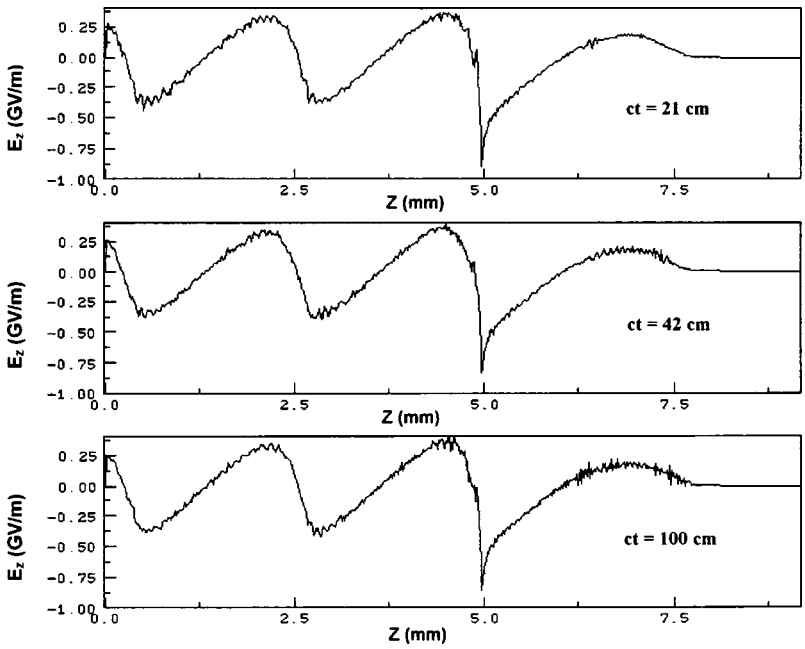

FIG. 13. Longitudinal wakefield at distances of 21, 42, and 100 cm into the plasma.

$$\frac{\lambda_\beta}{2} = \pi\left(\frac{\gamma m c^2}{2\pi n_o e^2}\right)^{1/2}, \tag{2}$$

where λ_β is the wavelength of a single particle's betatron motion, and $\lambda_\beta/2$ is the wavelength for the beam envelope. For our example $\lambda_\beta/2$ is approximately 40 cm. The head of the beam has a longer and position dependent betatron wavelength. The phase mixing of the betatron oscillations at the head of the beam is also visible.

In Fig. 14 the upper and lower plots are at the minimum and maximum of the oscillation at the propagation distances at $\lambda_\beta/4$ and $3\lambda_\beta/8$, respectively, where they would be expected according to Eq. (2). By adjusting the length of the plasma cell, the electron beam can be made to exit with approximately the same radius and angle at which it entered. This condition of transverse transparency of the plasma as an optical element will be exploited in E-157 (to facilitate diagnostics). We note that in practice this condition can only be achieved approximately because the betatron wavelength is energy dependent [see Eq. (2)], and there is energy spread in the beam.

The beam becomes incredibly small at the pinches of the betatron oscillations. From the envelope equation of the beam,

$$\sigma'' + K\sigma = \varepsilon^2/\sigma^3, \tag{3}$$

with $K = 2\pi n_o e^2/\gamma m c^2$. We integrate once to obtain $\sigma_{\min} \sim 0.35\,\mu$m for our parameters. In the simulations, $\sigma_{\min}$ is about 2.6 μm. Differences may be due to aberrations caused by numerical errors inside the first radial cell (the beam at the pinch becomes much smaller than the cell size of 17 μm).

Next we explore the possibility of eliminating the betatron oscillations by matching the beam and plasma β functions [19]. From Eq. (3) we see that σ'' will be zero if $K\sigma = \varepsilon^2/\sigma^3$. This is the matched beam condition in which the balance between the plasma focusing and the beam's thermal pressure leads to a nearly constant radius solution rather than betatron oscillations. To test this expected behavior, we spoiled the beam emittance to achieve the matching condition (experimentally this could be done with a solid foil of appropriate thickness placed in the beam path). We note that we may also have achieved the matching condition by reducing the beam spot size. However, this would require a finer grid size resolution and a much longer computational time. The result is shown in Fig. 15. Snapshots of the beam at the same distances as in Fig. 14 show the beam propagating with a relatively fixed radius.

Figure 16(a) shows the energy distribution of the beam particles at the end of the simulation. There are three important features that should be noted in this plot. The front part of the beam did not change energy, the middle part of the beam lost about 200 MeV, and particles in the tail of the beam gained energies up to 700 MeV. In the distribution plot, the highest bin shown is at 700 MeV, and contains $\sim 2\times 10^8$ particles. This peak energy gain is about 1 GeV

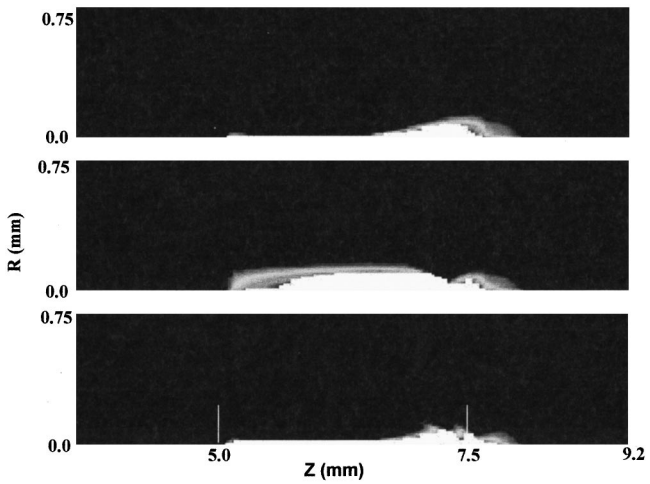

FIG. 14. Contour plot of bunch charge density in real space at the same three distances of propagation as in Fig. 13 (21, 42, and 100 cm), showing the betatron oscillations of the beam. $\varepsilon_N = 60$ mm mrad.

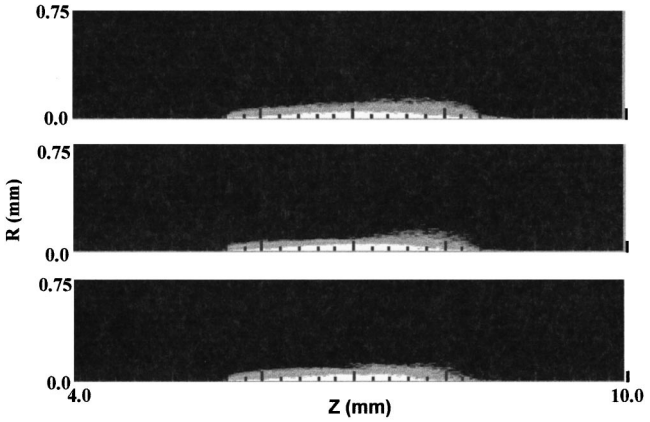

FIG. 15. Contour plot of the bunch charge density in real space at three distances ($z=21$, 42, and 100 cm) for an emittance-spoiled beam showing a lack of betatron motion. Parameters are as in Fig. 14, except $\varepsilon_N=3000$ mm mrad.

compared to what would be predicted from the product $E\cdot\ell$ where $\ell=1$ m and E is the value of the peak electric field in the short simulations. Also shown in Fig. 16(b) is a distribution plot found from the product of the early time electric field experienced by each particle times a distance of 1 m. Figure 16(c) shows the corresponding result if all beam particles were to experience the on-axis field. These results show that multiplying the on-axis electric field by a length of the run overestimates the final energies by approximately 10%. The difference between Figs. 16(b) and 16(c) shows the effect of the reduced accelerating force experienced by beam particles outside of the blowout region.

VI. DISCUSSION

Based on linear theory and computer simulation, we explored the physics of a meter-long plasma wakefield accelerator experiment. A number of widely used PIC models

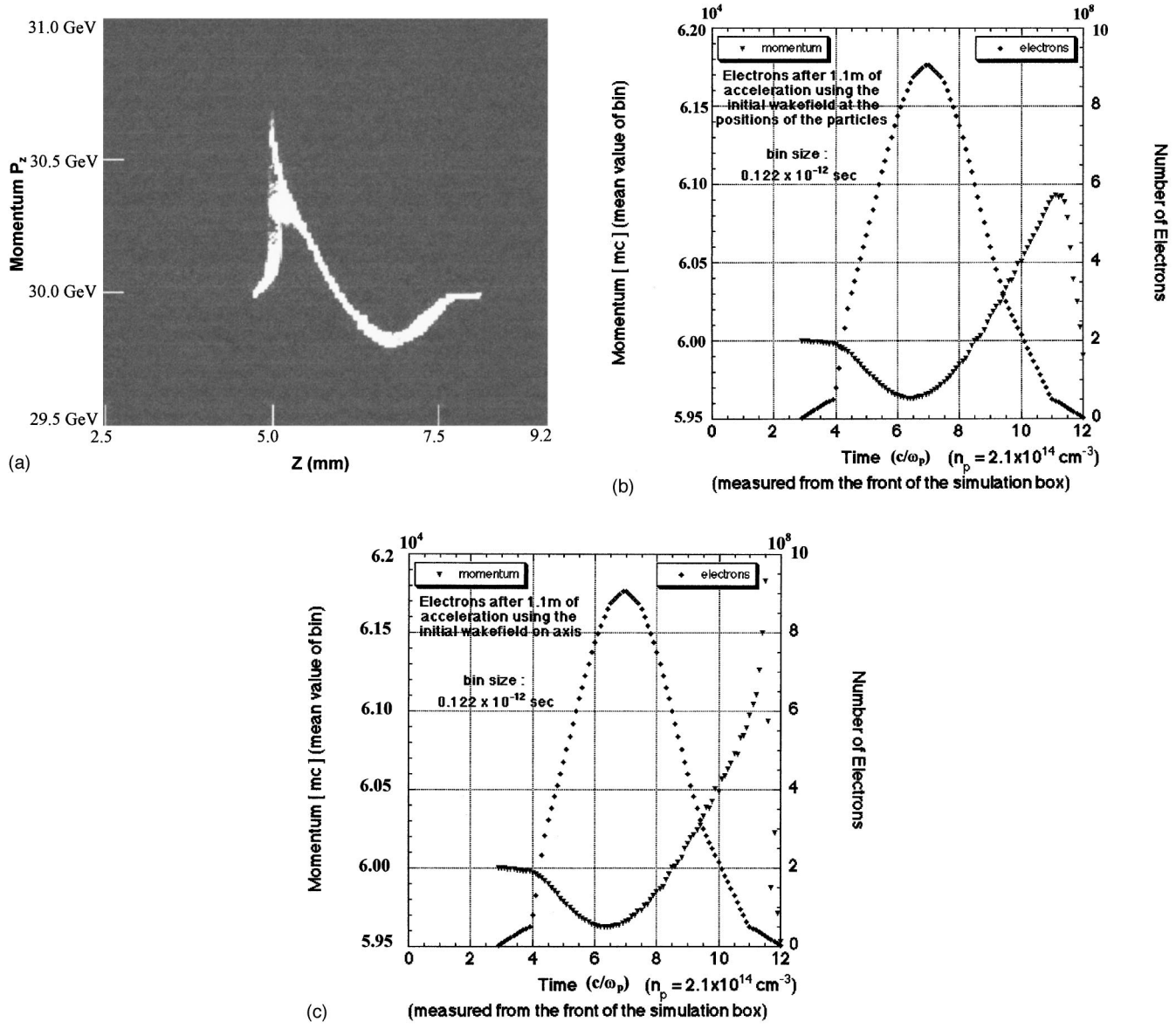

FIG. 16. Contour plot of longitudinal phase space density (a) at the end of a 1-m plasma, (b) found from the initial wakefield E_z at the initial particle positions times 1 m, and (c) from the initial wakefield on axis times 1 m. Bins were 0.122 ps in time.

were benchmarked against each other for short distances, and advanced algorithms were used to enable simulation of full meter scales. Results showed that energy gains of several hundred MeV over a meter are possible with present SLAC beam parameters. The nonlinear enhancement of the transformer ratio and transverse betatron motion of the beam were also investigated. In principal, the beam can be matched either by decreasing its spot size or by increasing its emittance.

In a real experiment, some deviations from the idealization of this 2D model may be expected. Correlated energy spread of the beam has not been included, and will introduce some phase mixing of the betatron oscillations. Asymmetry in the x and y beam emittance and some transverse instabilities such as hosing require 3D simulation. We comment briefly on instabilities in the beam plasma interactions modeled in this paper. The major concern in the blowout regime is the growth of the electron hose instability [17]. This instability arises when there is a head-tail offset in the beam. The head causes a plasma oscillation in the plasma surrounding the blowout region that feeds back on the tail amplifying its offset. Typically the growth becomes very large when the beam is longer than the plasma period. A similar symmetric sausaging instability may also be possible. In the simulation presented here, the beam is coaxial, and hence the noise source for the hosing is small. Furthermore, for typical parameters we model, the beam is short so that one may expect only few e foldings of growth [19]. Preliminary 2D simulations we have done with a head-tail offset have not shown appreciable growth. In preliminary 3D simulations, electron hosing is observed in the higher density cases.

Finally we comment on the validity and implications of the scaling law given in Sec. II. Although derived from linear theory, the basic scaling of maximum wake amplitude with N/σ_z^2 seems to hold in PIC simulations well into the nonlinear blowout regime. The strong dependence on bunch length suggests that far higher accelerating fields could be generated in the PWFA scheme with modest reductions in the bunch length. These are the subjects of future work.

ACKNOWLEDGMENTS

We wish to thank Larry Ludeking and Mission Research Corporation for their support on the use of MAGIC. MAGIC simulations and research were supported by AFOSR (Grant No. F49620-95-1-0248). This work was also supported by the U.S. DOE under Contract Nos. DE-FG03-92ER40745, DE-FG03-98DP00211, and DE-FG03-92ER40727, the NSF under Grant Nos. ECS-9632735 and DMS-9722121, and LLNL under Contract No. W07405-ENG48. This work was performed while one of the authors (T.K.) was on leave at the Stanford Linear Accelerator Center. Useful discussions with D. Gordon, C. Schroeder, J. S. Wurtele, and the members of the E-157 collaboration (R. Assmann, P. Chen, F. J. Decker, E. Esarey, M. Hogan, R. Iverson, T. Kotseroglou, P. Raimondi, T. Raubenheimer, S. Rokni, R. H. Siemann, D. Walz, D. Whittum, C. Clayton, C. Joshi, K. Marsh, S. Wang, S. Chattopadhyay, P. Catravas, W. Leemans, and P. Wolfbeyn) are gratefully acknowledged.

[1] R. Assmann *et al.* (unpublished).
[2] J. B. Rosenzweig, B. Breizman, T. Katsouleas, and J. J. Su, Phys. Rev. A **44**, R6189 (1991); D. Whittum, Ph.D. thesis, UC Berkeley, 1990.
[3] T. Katsouleas, S. Wilks, P. Chen, J. M. Dawson, and J. J. Su, Part. Accel. **22**, 81 (1987).
[4] T. Katsouleas, J. J. Su, C. Joshi, W. B. Mori, J. M. Dawson, and S. Wilks (unpublished).
[5] T. Tajima and J. M. Dawson, Phys. Rev. Lett. **43**, 267 (1979).
[6] N. Barov and J. B. Rosenzweig, Phys. Rev. Lett. **49**, 4407 (1994).
[7] B. Goplen, L. Ludeking, D. Smithe, and G. Warren, Comput. Phys. Commun. **87**, 54 (1995).
[8] H. R. Lewis, J. Comput. Phys. **10**, 400 (1972).
[9] K. C. Tzeng, W. B. Mori, and C. D. Decker, Phys. Rev. Lett. **76**, 3332 (1996).
[10] J. J. Su, Ph.D. Thesis UCLA, 1989.
[11] R. Hemker *et al.* (unpublished).
[12] S. Lee, T. Katsouleas, in *Advanced Accelerator Concepts, Baltimore, 1998*, edited by Wes Lawson, Carol Bellamy, and Dorothea F. Brosius, AIP Conf. Proc. No. 472 (AIP, New York, 1999).
[13] P. Chen, J. J. Su, J. M. Dawson, K. L. F. Bane, and P. B. Wilson, Phys. Rev. Lett. **56**, 1252 (1986).
[14] J. B. Rosenzweig, B. Breizman, T. Katsouleas, and J. J. Su, Phys. Rev. A **44**, R6189 (1991).
[15] R. D. Ruth, A. W. Chao, P. C. Morton, and P. B. Wilson, Part. Accel. **17**, 171 (1985).
[16] K. V. Lotov, Phys. Plasmas **3**, 2753 (1996).
[17] D. H. Whittum, J. Phys. **30**, 1007 (1997).
[18] T. Katsouleas, Phys. Rev. A **33**, 2056 (1986).
[19] B. J. Duda, R. G. Hemker, K. C. Tzeng, and W. B. Mori, Phys. Rev. Lett. **83**, 1978 (1999).